Supplemental materials and methods

Viability and behavioral tests

In the viability test, 200 embryos were plated on a Petri dish containing 3% agarose supplemented with grape juice and with yeast paste. Subsequently, 1st instar larvae were moved to vials with a standard medium. Individuals, achieving each stage of development (3rd larval instar, pupae, imago) were quantified. Behavioral assays were carried out on fifteen 3rd instar larvae per genotype and repeated 3 times for each individual. For all locomotor assays larvae were placed for at least 120s on a Petri dish filled with solidified 3% agarose for adaptation before being tested. In the righting assay, individuals were placed on a Petri dish with 3% agarose on a dorsal position and the time needed to reverse to a ventral position was measured. For the journey test a 2 mm wide, 5 mm deep and 60 mm long track was created on a Petri dish containing 3% agarose. Fresh yeast paste was placed behind the end line as a stimulus. Larvae were placed on the test track and the time taken to crawl 50 mm distance was recorded. In motility test larvae were crawling on a Petri dish with 3% agarose and the number of peristaltic movements were counted during 30 s.

Muscle morphology measurements

VL3, VL4 and SBM muscles of abdominal segments 3 or 4 were analysed in 15-22 dissected and fixed 3rd instar larvae, as described above. Observations of muscle morphology, as well as measurements of muscle length, diameter, number and size of sarcomeres were carried out on muscles stained with phalloidin. Muscle nuclei were visualized by anti-Mef2 antibody. The fibre contractility index (CI) was calculated from following formula: CI = (size of relaxed fibres – size of contracted fibres)/size of relaxed fibres. FV300 (Olympus) confocal microscope was used for imaging and Fluoview software (Olympus) for muscle measurements. Statistical analyses were carried out using the GraphPad Prism5 software. T-test non-parametric or one-way ANOVA were used for phenotypes comparison. The results are reported on the graphs as a standard error of a mean and $P<0.05$ is considered as statistically significant.

RT-PCR

To obtain *Drosophila* cDNA, total RNA was extracted from 50 3rd instar larvae (WT and Mef> CryAB-RNAi, using a TRIzol reagent (Invitrogen). The remaining DNA was removed by RQ1 DNAse (Promega). 2 µl of each RNA were used for reverse transcription, performed with the Superscript III First strand Synthesis System (Invitrogen) according to manufacturer's instructions. To compare the level of *cryAB* expression in selected fly strains, 2 µl of reverse transcription products (described above) were amplified via PCR, by using following pairs of primers: forward, 5'-TCCGTAGTGCCACTGATGTTC-3' and reverse, 5'-CTAGGCGGTGGAGGTCTCC-3'. As a control *gapdh1* was used, whose expression remains at a constant level. All the DNA amplifications were obtained with a Taq DNA polymerase (Invitrogen) according to manufacturer's instructions.

Heart physiological analysis

Anesthetized flies with fly nap (Carolina Biol., Corp.) were dissected to expose the heart for filming according to previously described protocols (Fink et al., 2009). These beating heart movies were taken at rate of about 130 frames per second using Simple PCI software (Compix, Sewickley, PA). We use MatLab-based image analysis program to quantify and generate cardiac parameters measurements (Fink et al., 2009). M-modes illustrate movements

of the heart tube edges in Y-axis over time in X-axis, generated by excising and aligning a single pixel-wide from successive movie frames. Heart periods are defined as the time between the ends of two consecutive diastolic intervals. We used Prism software–one way ANOVA analysis and Tukey test to perform the statistics on 20 flies for each genotype.

Generation of *UASp-Cher90_GFP* line

To generate *pUASP-Cher90* we cloned a NotI-EcoRI cheerio fragment with an EcoRI-XbaI mGFP6 fragment into the *attB-UASP* vector (kindly provided by Beat Suter) cut NotI-XbaI. We used the following primers to generate the cheerio fragment from the EST RE60544 (DGRC):
ATATATGCGGCCGCATGCCTAGCGGTAAAGTAGACAAACCCGTGAT and
ATATATTCTAGAGAATTCCACATCGATCTGGAATGGGGAGCCGGGTATATGC;
We used the following primers to generate the mGFP6 fragment:
ATATATGAATTCCCCTCGAGCTCATCGATGAGTAAAGGAGAAGAA and
TATATATCTAGATCAAGCTTTGTATAGTTCATCCATG.
The construct was sequenced and integrated into the attP landing site 51D (Bischof et al., 2007).

Generation of *UASp-Venus-dCryAB*, *UASp-Venus-dCryABR120G* and *UASp-Venus-dCryAB ABDmut* lines

For plasmid construction *dCryAB* coding sequences were amplified on cDNA obtained by reverse transcription of total RNA from 3rd instar larvae. PCR reaction using a high-fidelity DNA polymerase (Phusion, Biolabs) was performed with the following pair of primers, containing XbaI and BamHI restriction sites (underlined):
Forward 5'-ATATCTAGATCCGTAGTGCCACTGATGTTC-3';
Reverse 5'- TATGGATCCCTAGGCGGTGGAGGTCTCC-3'.
Amplified dCryAB PCR product was digested with BamH1 and Xba1 and cloned into pUASp-PL-Venus vector which was then injected into a w^{1118} embryos to produce transgenic flies, a step performed by the Fly Facility platform (www.fly-facility.com Clermont-Ferrand, France).
To introduce R120G and ABDmut point mutation into dCryAB we applied PCR-based mutagenesis. Two overlapping PCR products carrying point mutation were first generated with following pairs of primers (mutated nucleotides are underlined and in bold):
Forward 5'-ATATCTAGATCCGTAGTGCCACTGATGTTC-3'
Reverse R120Gmut 5'-AGCTGGTAGCGTC**C**GGAGAACTGGCGGG-3',
Reverse ABDmut 5'-GTCACATCGTCCCTCTCCTCC**T**ATGGCCTGCTGACCATCAAGGC-3'
Forward ABDmut 5'-GCCTTGATGGTCAGCAGGCCAT**A**GGAGGAGAGGGACGATGTGAC-3'
Forward R120Gmut 5'-CCCGCCAGTTCTC**C**GGACGCTACCAGCT-3'
Reverse 5'- TATGGATCCCTAGGCGGTGGAGGTCTCC-3',
2 µl of each PCR product carrying point mutation were mixed in 16 µl of water, heated to 99°C and annealed by cooling down to 37°C during 25 min. 2 µl of annealed PCR products were then used for final PCR amplification with Forward and Reverse primers. Cloning of mutated dCryABR120G and dCryAB ABDmut and generation of transgenics were as for the wild type UASp-Venus-dCryAB.

Mass spectrometry

We applied Mass Spectrometry (MS) to identify the dCryAB interacting proteins. Immunoprecipitation was performed as described below using dCryAB antibody on cytoplasmic protein extract from the dissected wild type larvae. The immunoprecipitated protein complexes were subjected to SDS-PAGE separation and Coomassie staining to

visualize bands of interest. Proteins ranging from 30 to 170 kDa were excised from the gel and analyzed by a specialized Mass Spectrometry and Proteomics Platform (MSPP, SupAgro INRA, Montpellier).

TEM

Dissected larvae (as described above) were fixed in 2,5% glutaraldehyde in 0,1M phosphate buffer, 3 times washed in phosphate buffer for 15 min, incubated over night and again washed 3 times. Material was post-fixated for 90min in the mixture of osmium tetroxide and potassium ferricyanide in the ratio 1:1. After dehydration in alcohol series (50%, 70%, 90%, 100%, 100%), material was embedded in a mixture acetone-epoxy resin in the ratio 1:1 and incubated for 24h in a very tight dish. The dish was opened for at least 7h for acetone to evaporate. Polymerization of material embedded in epoxy resin was performed during 24h at 45ºC and subsequently for 3 days at 60ºC. Ultrathin sections were observed in electron microscope Zeiss EM 900.

Immunogold

Dissected larvae (as described above) were fixed in 1:1 mixture of 0,5% glutaraldehyde and 4% paraformaldehyde in a PBS, at RT for 1,5h. Than the material was postfixed in 2% paraformaldehyde, at 4ºC overnight, washed in PBS with 0,5% TritonX100 (PBT) and dehydrated with graded ethanol series. After dehydration specimens were infiltrated in mixtures of 85% ethanol and LR White (London Resin Company Ltd) (2:1), (1:1), (1:2) 1h for each series. Then the material was infiltrated in two times with pure LR White for 12h at RT and once overnight at 4ºC and embedded in LR White and polymerized at 59ºC for 24h. Ultrathin sections were cut using an ultramicrotome (ReihertUltracut E). Ultrathin sections were preincubated for 2 h in 1% BSA in PBS. Then sections were incubated with primary antibodies: mouse anti-β-actin 1:10 and rat anti-dCryAB 1:500 at 4ºC overnight. After rinsing several times in PBT the material were incubated with secondary antibodies conjugated with gold particles. After washing in PBT, sections were contrasted with lead citrate for 2 min and analyzed using transmission electron microscope Zeiss EM 900.

Bioinformatics search for homologues

To compare amino acid sequences associated to dCryAB and CryAB, we used MUCLE (Multiple Sequence Comparison by Log-Expected) with default settings (McWilliam et al., 2013). We visualized the result with Jalview2 (Waterhouse et al., 2009) highlighting equivalences in red. Phylogenetic tree was built considering amino acid sequences of dCryAB, CryAB, Hspb1 and Hspb8 and those of some of their different homologues in various vertebrate and non-vertebrate species. We used phylogenetic analysis « One Click » pipeline available on (http://www.phylogeny.fr) to manage the different building steps and generate the final tree.

Supplemental figure legends

Figure S1. Double EM immunogold staining for dCryAB and actin showing that immunogold dots for dCryAB (18 nm of diameter) localize mainly to the Z-band but are also detected within the M-band. Note that small immunogold dots of 10 nm of diameter detecting actin are found at the Z-band. Scale bar 300 nm.

Figure S2. Effects of muscle targeted RNAi attenuation of dCryAB using VDRC 107305 line. (A) Lateral view of wild type dissected 3rd instar larval muscles from one hemisegment stained with phalloidin. Note altered pattern of sarcomeric actin suggesting disruption of Z-bands (arrowheads). (B) Statistical representation of muscle defects observed in examined *Mef>dCryAB-RNAi* larvae. (C) No significant changes in sarcomere size have been observed. (D) Significantly reduced number of sarcomeres observed in 3 different muscles (VL3, VL4 and SBM) in 3rd instar larvae with muscle-specific attenuation of dCryAB. (E-H) Affected contractility and muscle performance tests showing reduced motility of *Mef>dCryAB-RNAi* larvae. (I) No apoptotic events can be detected in *Mef>dCryABRNAi* muscles as judged by the activated Caspase 3 staining. Arrow points to cells that undergo apoptosis in the analyzed 3rd instar larvae preparation. Significant differences were determined by t-Student test. Asterisks indicate statistical level of significance of observed differences: *p<0,1, **p<0,5, ***p<0,001. Scale bar 40 μm.

Figure S3. Muscle targeted expression of dCryAB carrying mutated actin binding domain (ABD) affects sarcomeric actin pattern and nuclei positioning. The alignment of wild type and mutated amino acid sequence of dCryAB actin binding domain are shown. Mutated residue is in red and highly conserved residues are in bold (refer to Mounier and Arrigo, 2002). Arrows in (A) point to irregular actin pattern. Arrowheads in (A') indicated abnormally located dCryAB with mutated ABD whereas asterisk point to the area in which dCryAB-ABDmut displays a diffused pattern and is not detected in sarcomeres. Arrowheads in (A") denote clustered nuclei. Scale bar 50 μm.

Figure S4. Additional muscle defects observed after attenuation of *dCryAB*. (A) Muscle splitting (yellow arrowhead) with partial loss of splitted myofibrils. (B) Complete loss of a muscle. Arrowheads indicate position of extremities of lacking segment border muscle. Scale bar 40 μm. (C) Slightly but significantly reduced number of sarcomeres observed in 3

different muscles (VL3, VL4 and SBM) in 3rd instar larvae with muscle-specific attenuation of *dCryAB*. (D) No significant changes in sarcomere size have been observed. (E) *Mef>dCryAB-RNAi* animals display increased lethality at all developmental stages tested. Significant differences were determined by t-Student test. Asterisks indicate statistical level of significance of observed differences: *p<0,1, **p<0,5, ***p<0,001. Error bars indicate SEM.

Figure S5. dCryAB does not physically interact with Msp300. Western blot from IP experiment with anti-dCryAB on protein extract from 3rd instar larvae. Anti-Msp300 antibody was used to reveal immunoprecipitation reaction. Notice high molecular weight Msp-300 detected in the protein extract (Input) but not in the IP sample.

Figure S6. Bar graph representations of changes in heart parameters upon cardiac-restricted expression and knockdown of dCryAB. (A, B) Plot of mean systolic (A) and diastolic (B) intervals indicates shortening in contraction and relaxation phases for dCryAB lines. (C) Heart diastolic diameters for 1 week-old flies. Note the dilated diameters across the heart tube in $dCryAB^{R120G}$ flies. (D) Percent fractional shortening shows significant decrease when driving R120G dCryAB at 1 week old, in comparison to controls. Movies were taken from 20 flies for each genotype. Significant differences were determined by one-way ANOVA ([*] P<0.05; [**] P<0.005; [***] P<0.0005). Error bars indicate SEM.

Figure S7. Genetic interactions of dCryAB and cheerio and their impact on sarcomeric pattern. (A-A") Simultaneous RNAi knockdown of dCryAB and cheerio leads to misalignment of myofibrils (arrows in A) associated with severely affected sarcomeric actin and kettin patterns. High kettin level (asterisk in A') is detected in the sarcomeres displaying reduced/fuzzy actin (asterisk in A), a phenotype that has not been observed in muscles in which only dCryAB has been attenuated (see Fig. 4B). (B-B") Overexpression of dCryAB in cherRNAi context partially rescues irregular/fuzzy actin patterns observed in muscle with attenuated cheerio (Fig. 7E). Notice that some myofibrils misalignment can still be observed but sarcomeric kettin distribution appears regular in this context (B'). Scale bar 40 μm.

Figure S8. Muscle targeted RNAi knockdown of Starvin leads to misalignment of myofibrils and affected nuclei position but has no influence on sarcomeric and perinuclear localization of dCryAB. Arrows point to misaligned myofibrils and accumulation of dCryAB. Arrowheads indicate clustered nuclei. Scale bar 40 μm.

References:

Mounier N, Arrigo AP. Actin cytoskeleton and small heat shock proteins: how do they interact? Cell Stress Chaperones. 2002 Apr;7(2):167-76.

Table S1. Proteins identified by Co-IP with CryAB

Protein	**No. of matches/peptides**	**Protein**	**No. of matches/peptides**
Tropomyosin 1	108/19	α-actinin	18/12
Actin 57B	93/18	GlyP	18/10
Actin 87E	86/17	Ca-P60A	17/10
Actin 5C	66/16	PyK	16/12
Tropomyosin 2	61/11	Ef1 alpha 48D	16/7
Impl 3	47/15	Mp20	12/6
Arginine kinase	43/18	Pgi	11/6
Paramyosin	42/20	Pgm	10/8
Gapdh2	38/14	Hsp70	10/7
Gapdh1	33/11	Cheerio/dfilamin	9/6
MHC	25/19	Ef2b	8/6
Hsp60	24/13	Trip1	8/6

Supplementary figures

Figure S1

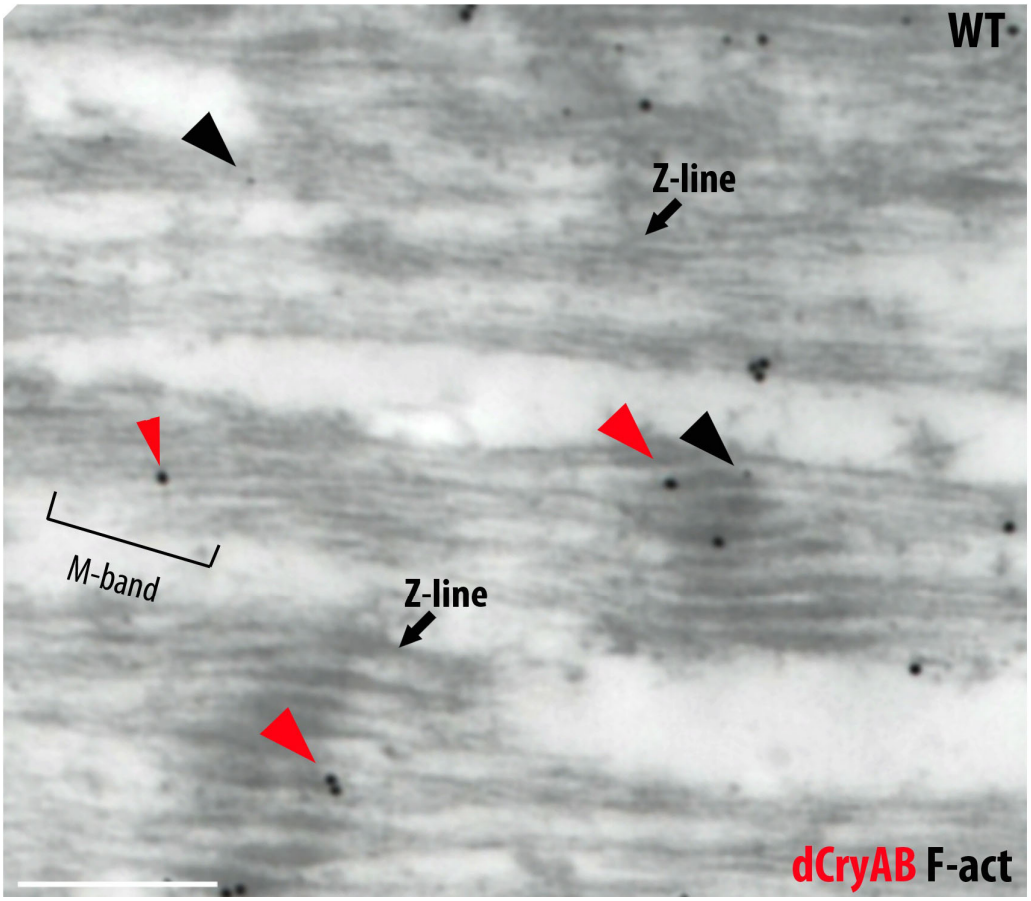

Figure S2

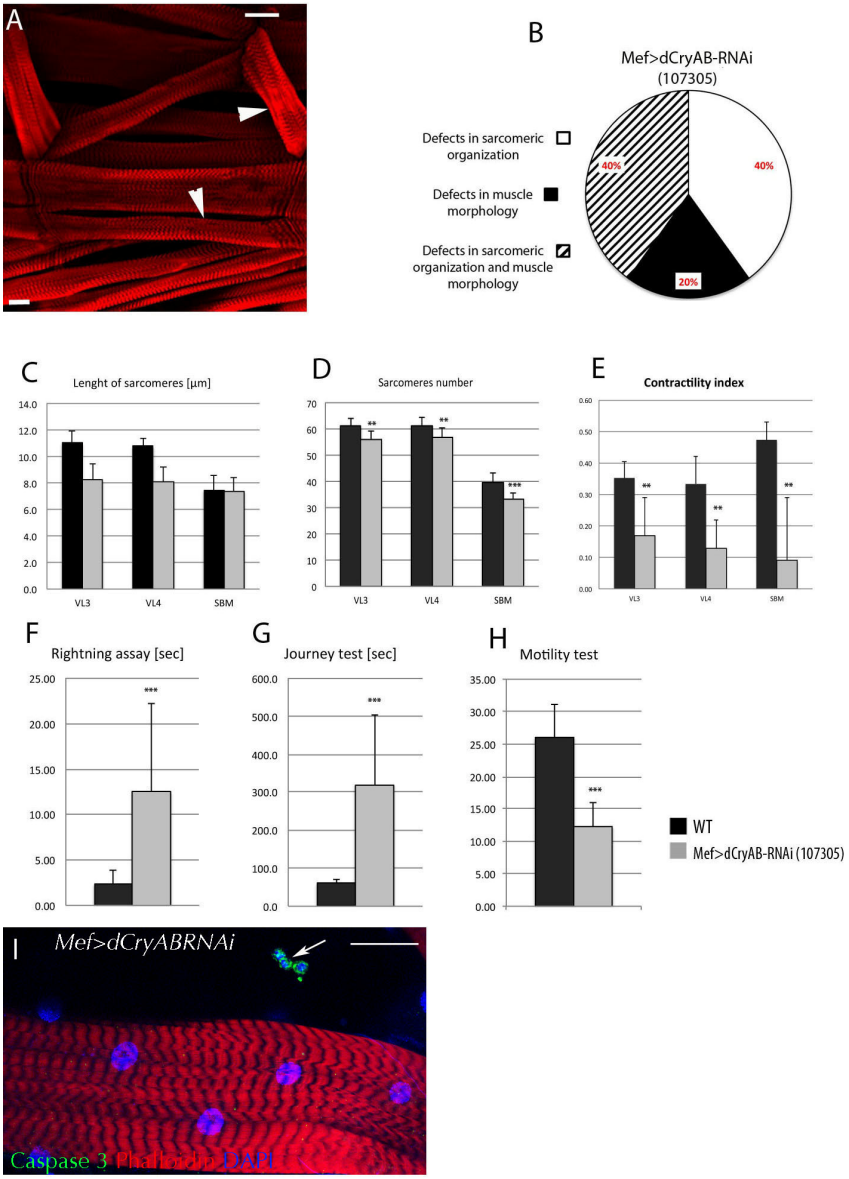
A
B
Mef>dCryAB-RNAi
(107305)
Defects in sarcomeric organization
Defects in muscle morphology
Defects in sarcomeric organization and muscle morphology
40%
40%
20%
C
Lenght of sarcomeres [µm]
VL3
VL4
SBM
D
Sarcomeres number
E
Contractility index
F
Rightning assay [sec]
G
Journey test [sec]
H
Motility test
WT
Mef>dCryAB-RNAi (107305)
I
Mef>dCryABRNAi
Caspase 3 Phalloidin DAPI

Figure S3

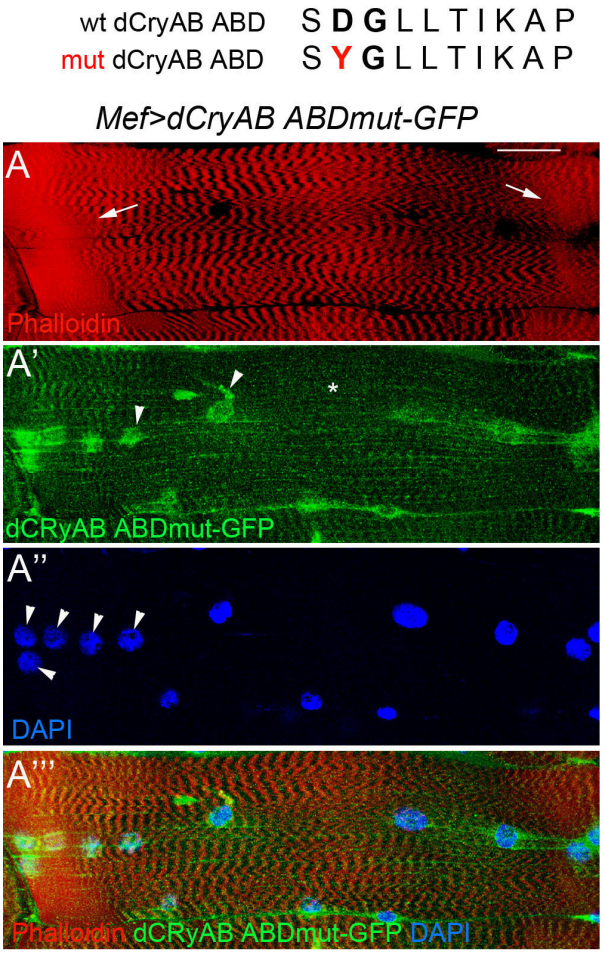
wt dCryAB ABD S D G L L T I K A P
mut dCryAB ABD S Y G L L T I K A P
Mef>dCryAB ABDmut-GFP
A
Phalloidin
A'
dCRyAB ABDmut-GFP
A''
DAPI
A'''
Phalloidin dCRyAB ABDmut-GFP DAPI

Figure S4

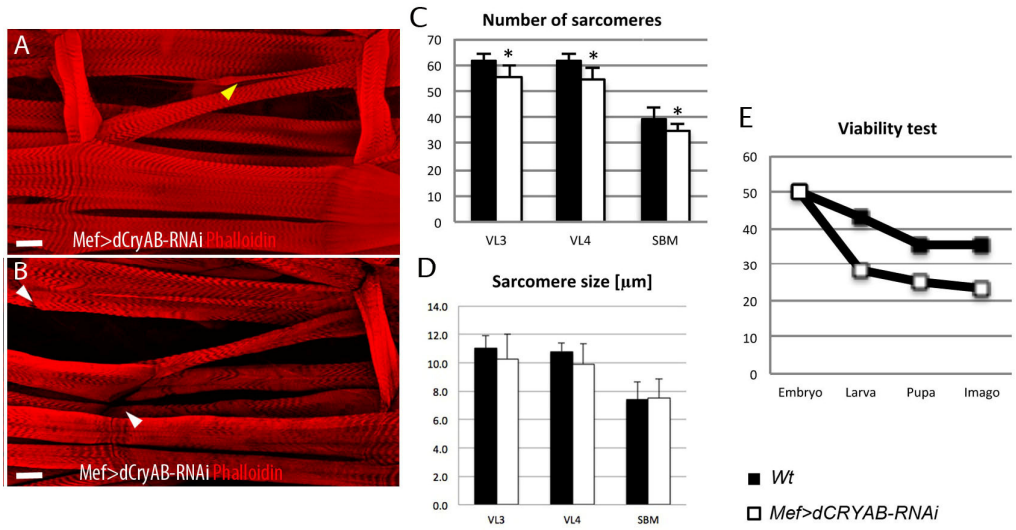

Figure S5

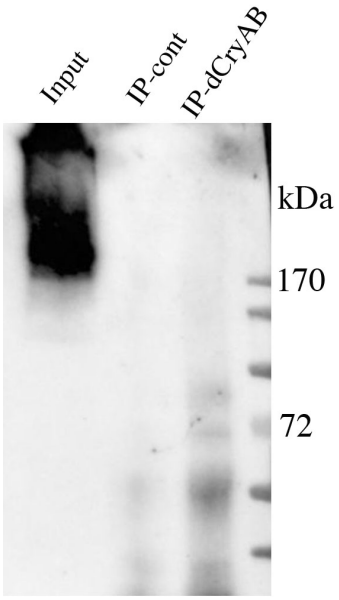

Figure S6

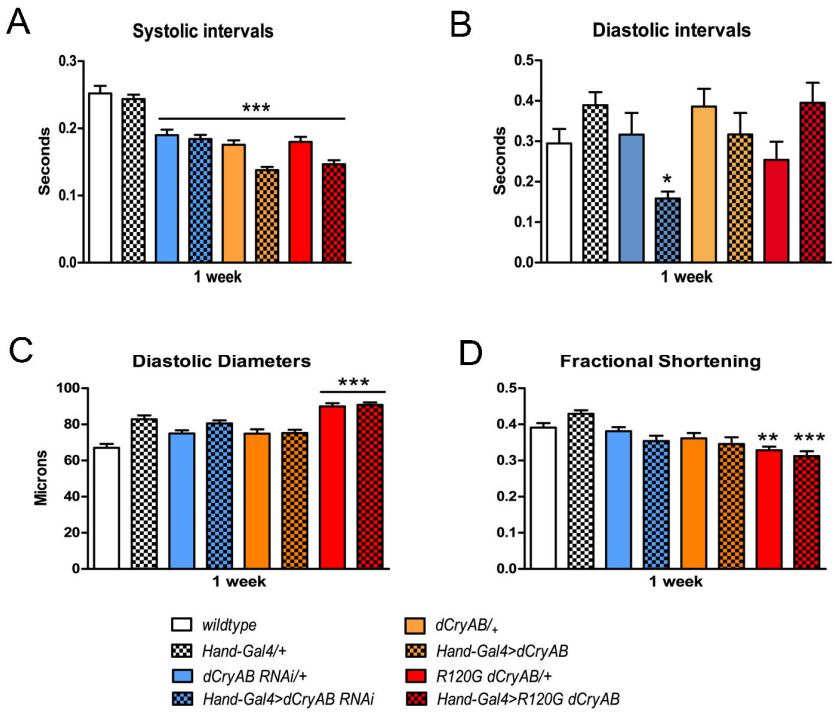

Figure S7

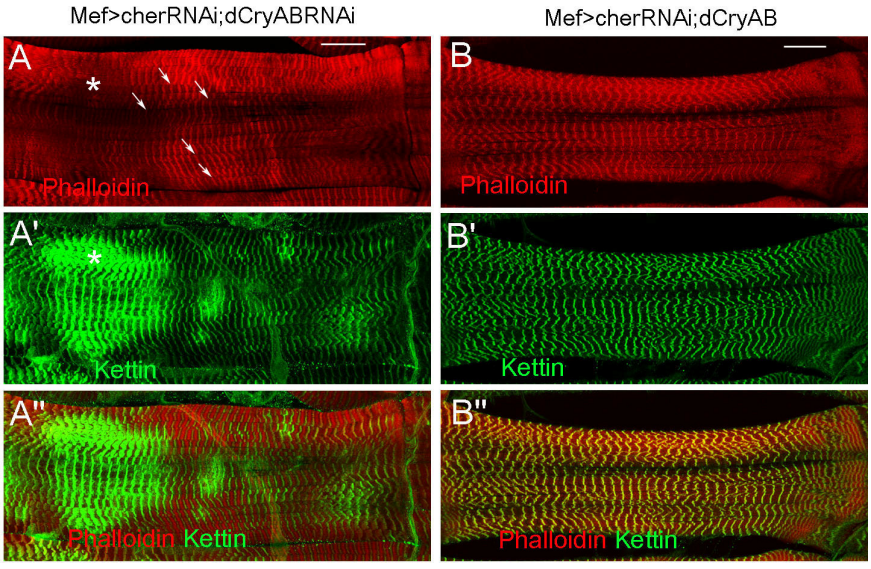

Figure S8

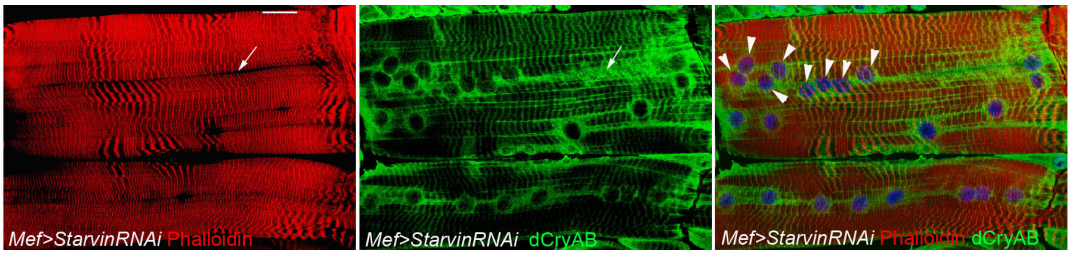
Mef>StarvinRNAi Phalloidin
Mef>StarvinRNAi dCryAB
Mef>StarvinRNAi Phalloidin dCryAB